JOURNAL OF PROPULSION AND POWER
Vol. 13, No. 2, March–April 1997

Combustion Initiated by a Porous Ceramic Regenerator in a Reciprocating Engine Environment

Steven Sepka* and Francisco Ruiz†
Illinois Institute of Technology, Chicago, Illinois 60616

This paper presents the experimental results of thermally initiated, premixed combustion by a porous ceramic matrix physically located above the cylinder bore inside a combustion chamber. This article's purpose is to show the ability of the matrix to act as a combustion initiator and to show its ability for promoting complete combustion. Surface temperatures and exhaust gas composition were recorded using thermocouples and a nondispersive infrared gas analyzer. Results show that complete combustion at mass air–fuel ratios above 20 were possible with products (on a dry, molar basis) of CO below 0.35%, CO_2 above 11.5%, and unburned hydrocarbon emissions below 40 ppm. When the ignition source was the ceramic surface (unaided by spark ignition) there was no noticeable carbon particulate buildup on its surface. Based on these results, ceramic matrix surface ignition shows potential for becoming a better ignition source than an ordinary electric spark for lean-burning engines.

Introduction

THIS paper is based on previous experimental work[1,2] of an engine concept named the regenerative engine (see Fig. 1). The experimental findings presented here are an initial step to quantify the ability of a porous ceramic matrix to promote combustion in an experimental setup not too unlike those of conventional spark ignition (SI) engines. What is unique to this arrangement is the porosity of the matrix, a property that allows combustion gases to transfer heat more effectively than by exterior surface contact alone, resulting in surface temperatures above the ignition temperature of the fuel. This engine did not produce work, but was used because it allowed a reciprocating flow of reactants and products through the porous matrix without the added complexity of an intake and compression stroke.

Surface ignition in combustion chambers is not a new phenomenon. Sir Davy's discovery of catalytic (surface) combustion[3] of coal–gas and air mixtures by a heated platinum wire occurred in 1817. Today, catalytic combustion is evidenced by a direct-injection diesel engine using a glow plug or by the autoignition of gasoline–air mixtures by carbon hot-spots in the combustion chamber. Systems using nonporous ceramics for combustion initiation have been shown to be possible,[4,5] as well as plug-flow porous-fiber gas burners having stationary reaction zones at the end of a wire matrix.[6] Our experimental setup, however, is the only one known by the authors to have a reciprocating flow of combustion products and reactants through the ceramic, leading to enhanced heat transfer and surface ignitability. An internal combustion (IC) engine using alcohol fuel and a nonporous ceramic insert for hot-surface-ignition has been shown to be possible.[7] However, at part load, the ceramic surface did not reach temperatures capable of promoting complete combustion, and a glow plug was needed as an ignition aid. The glow plug's required temperature for complete combustion was in excess of 915°C, a similar value to be shown in our experimental results.

Received Aug. 2, 1995; revision received Sept. 25, 1996; accepted for publication Sept. 25, 1996.

*Lecturer, Mechanical, Materials, and Aerospace Engineering Department, Engineering 1 Building, 3110 South State Street.

†Associate Professor, Mechanical, Materials, and Aerospace Engineering Department, Engineering 1 Building, 3110 South State Street.

For our system, the air–fuel (AF) mixture follows a four-stroke cycle split between the compression and expansion cylinders. The compression cylinder performs the carbureted intake and pumps the mixture (at about 2 atm) into the expansion cylinder via a transfer pipe with a one-directional check valve (to prevent flashback into the compression cylinder). The two-stroke expansion cylinder performs combustion and exhaust. When the mixture enters the expansion cylinder, it ignites on the surface of the ceramic (regenerator) matrix.

The phase difference between pistons was 67.5 deg for all tests, with the expansion piston leading the compression. This phase difference was set to allow the gases to fill the expansion cylinder. In both cylinders, the inlet valve is open for 180 deg of crank rotation with the exit valve closed, and the exit valve opens for the next 180 deg while the inlet valve remains closed. Electrical ignition was used for cold starting only. The spark was shut off once the matrix reached self-ignition temperatures (>800°C). Combustion occurred primarily above the regenerator with the matrix absorbing part of the heat of reaction. External motoring to crank the engine was required for all tests and the engine speed was kept constant at nearly 650 rpm.

Two cast iron plates were used to hold the regenerator matrix inside the combustion chamber. The regenerator has a disc

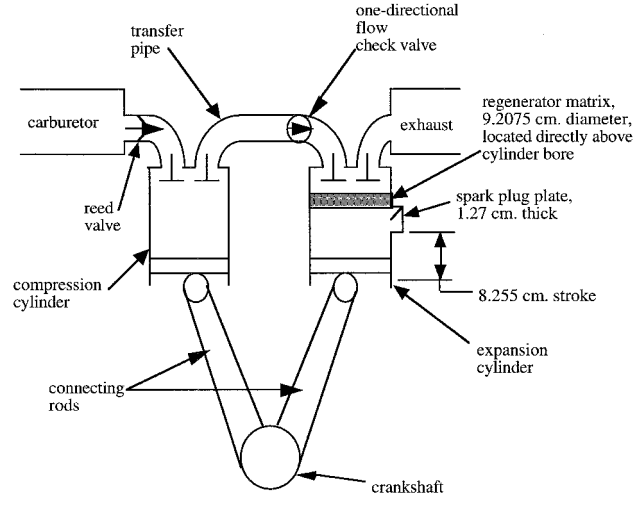

Fig. 1 Schematic diagram of test assembly.

Table 1 Bulk material properties

Material	Thermal diffusivity α, $m^2/s \times 10^6$	Thermal conductivity k, W/mK	Specific heat C, J/kg K	Density ρ, kg/m^3	Melting point, K
Honeycomb mullite	1.89	8.08	398	2600	1623
Mullite foam	11.9	36	765	3970	2083
ZTA foam	11.9	36	765	3970	1810

shape, 9.2075 cm (3.625 in.) in diameter and 1.9075 cm (0.75 in.) thick. An additional plate placed below the regenerator plates is used to hold a small spark plug for cold starting.

Two K-type flexible thermocouple probes were used for surface temperature measurements on either side of the matrix. For exhaust gas analysis, a four-gas nondispersive infrared (NDIR) analyzer probe was used. Unburned hydrocarbon output (in parts per million), %CO, and $\%CO_2$, were determined using NDIR, and $\%O_2$ was determined by polarography, which was accomplished in the same analyzer unit.

During testing, it was noticed that some of the fuel tended to leak into the oil pan of the compression cylinder. Since the exact flow rate was difficult to determine, it was decided to base all AF ratio calculations on the exhaust gas analysis.

Ceramic Material Testing

Three different types of matrix materials were tested: a 15-pore-per-inch (ppi) zirconia-toughened alumina (ZTA) reticulated cell regenerator, a 20-ppi mullite reticulated cell regenerator, and a 300 cells/in.^{2} uncoated cordierite honeycomb (UCH) monolith. A list of some bulk material properties is given in Table 1.

Experimental Procedure for Testing Ceramic Regenerators

Data were taken by holding either the intake airflow rate or the mass basis AF constant while physically changing the other. Changing the intake airflow rate with a constant AF shows the effect of throttling, and varying the AF with a constant intake airflow rate shows the effects of the stoichiometry.

A typical test begins with the engine at ambient temperature. Next, cranking the cold engine at open throttle, spark-induced combustion was heard. This combustion was very infrequent, and the rpm of the engine had to be kept below 900 rpm (caused, presumably, by convective cooling of the spark kernel not allowing the flame to propagate at a higher rpm). After approximately 2 min, depending on the type of matrix, the combustion noise changed to a rapid, repeatable pattern. At this point the matrix reaches temperatures able to ignite the intake mixture. The spark plug was then shut off and the intake throttled. Throttling was necessary to keep the matrix from reaching temperatures above the maximum operating temperatures of the thermocouple probes (1100°C). With no electric spark in the combustion chamber, all ignition originated at the regenerator matrix surface. All data were recorded under throttling with matrix surface ignition.

When readings stabilized, the following data were recorded: for surface temperatures, thermocouple output voltages and control room temperature (reference junction temperature), for emissions, %CO, $\%CO_2$, $\%O_2$, and ppm hydrocarbons (on a dry gas, mole fraction basis assuming all of the unburned hydrocarbons having the composition of gasoline), and finally for intake airflow, a manometer with test cell temperature and pressure readings for air density correction. To record temperature and emissions, the procedure was to wait until readings conformed to as small a variation as possible, quantify the range, and average several readings. Total run times lasted approximately 15 min. Experimental results will show that combustion occurs primarily above the ceramic matrix with our experimental setup, and that the aluminum head will begin melting when exposed to this heat release for times longer than 15 min.

These tests did not record the emissions of NO_x. If the matrix were to absorb part of the heat of reaction, thereby lowering the combustion products temperature, then the total output of NO_x is expected to decrease. This effect has been shown[8] to be true for radiant tube burners using reticulated ceramics to augment radial heat transfer. However, our system will preheat the intake air as it passes through the regenerator, leading to a rise in combustion product temperature and NO_x emissions. It has been shown[9] that this effect can be countered by increasing the equivalence ratio and reducing combustion product residence time to these temperatures and pressures (for our case, increasing the rpm).

Uncertainty of the Experiments

In all plots, either AF or intake airflow rate are held within a constant range (e.g., investigating the effects of throttling while holding the AF within the range of 13.7–14.7); the variation within the constant AF range induces some natural scatter in the data because not every test point was taken under identical conditions.

Averages for surface temperatures and emissions were taken from three to four sampled data. Our aim was simply to quantify the temperature levels found on the ceramic top and bottom surfaces, and the largest variation of the experimental data was ±43°C. This maximum variation, along with the error associated with each thermocouple (0.75% of reading from 0°C), gave a value of ±45°C to use as the deviation for surface temperature readings. Since all temperature measurements have the same uncertainty, the corresponding figures in this article do not show error bars. When measuring temperatures in excess of 1000°C, ±45°C corresponds to a 4.5% uncertainty.

Intake airflow measurements were taken with a manometer. A value of ±0.5 kg/h was the calculated uncertainty for all intake airflow measurements reported here. This value was obtained from the resolution of the manometer.

The gas analysis data have an uncertainty of 3% of reading. A rms analysis results in a deviation of ±0.3 for all AF calculations. This value was calculated by finding the largest variation in AF with a 3% change in each variable (%CO, $\%CO_2$, and $\%O_2$) and taking the square root of the sum of the squared differences of measured AF and its variation.

Experimental Results

It will be shown that the data can be grouped and their effects noted according to regenerator matrix surface temperature. To do this, the data were broken into two categories:

1) When the regenerator top surface temperature was above that of the bottom by at least 50°C (called top surface hotter).

2) When the bottom surface was at or near the top surface temperature (called both surfaces equal temperature).

Low throttling (intake airflow rates generally above 8.4 kg/h) and AFs between 14.7–20 lead to the top surface hotter case, and the opposite lead to both surfaces being nearly equal in temperature. Top surface hotter always occurred at temperatures able to ignite the intake flow before the gases had flown through the matrix, and was generally associated with good combustion. Good combustion was characterized by unburned hydrocarbon levels below 100 ppm, %CO below 0.2%, $\%CO_2$

above 11%, and $\%O_2$ between 3–5%. For low amounts of heat release it was possible to cause the regenerator bottom surface temperature to exceed the top, resulting in poor, incomplete combustion. This was probably the result of ignition delay or of reactions occurring only on the regenerator surface, unable to proceed into the homogeneous gas phase.

These effects are illustrated in Figs. 2–4. These tests with the 15-ppi ZTA matrix had the intake airflow rate varied between 6.5–11.5 kg/h while holding the AF to a nearly constant range of 13.7–14.7. The ZTA regenerator data are chosen because they typify the results obtained for the mullite and cordierite regenerators, respectively.

For the case of hotter top surface, the top surface temperatures were between 941–1017°C, and the bottom surface temperatures were between 830–895°C. For the case of both surfaces having nearly equal temperatures, the top surface temperatures were 856–910°C, and the bottom surface temperatures were 867–890°C.

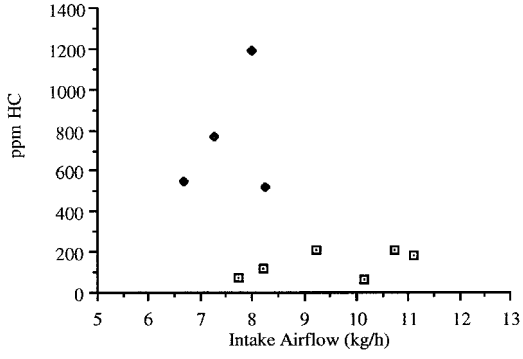

Fig. 2 Unburned hydrocarbon emissions for 15-ppi ZTA regenerator with AF 13.7–14.7. ⊡, top surface hotter and ♦, both surfaces equal temperature.

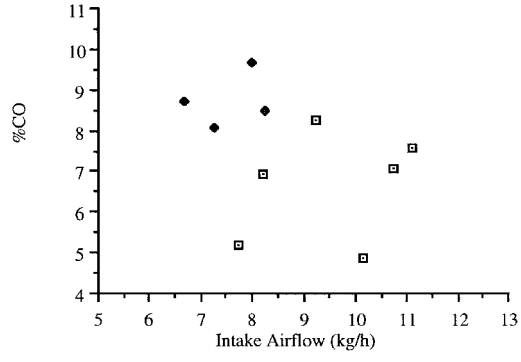

Fig. 3 Carbon monoxide emissions for 15-ppi ZTA regenerator with AF 13.7–14.7. ⊡, top surface hotter and ♦, both surfaces equal temperature.

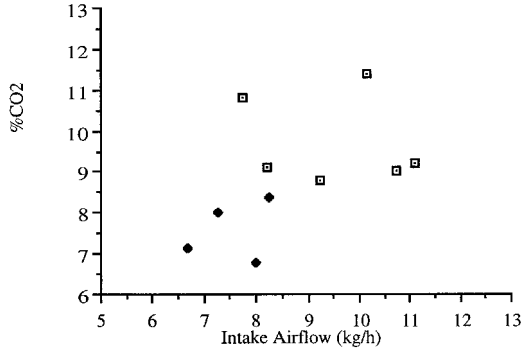

Fig. 4 Carbon dioxide emissions for 15-ppi ZTA regenerator with AF 13.7–14.7. ⊡, top surface hotter and ♦, both surfaces equal temperature.

Figure 2 illustrates the relation of surface temperatures to the emissions of unburned hydrocarbons. For top surface hotter, unburned hydrocarbon emissions were between 60–215 ppm. When both surfaces were of equal temperature, hydrocarbon output rose to 523–1186 ppm (an increase of nearly 600 ppm). Large variations in unburned hydrocarbons exist for this case with generally poor combustion.

Figure 3 illustrates the effects of surface temperatures on emissions of carbon monoxide (%CO). For top surface hotter, CO was between 4.86–8.26%; when both surfaces were of equal temperatures the CO value rose to 8.08–9.68%.

Figure 4 illustrates the effects of surface temperatures on emissions of carbon dioxide ($\%CO_2$). For top surface hotter, CO_2 was between 8.8–11.4%; when both surfaces were of equal temperatures the CO_2 value fell to 6.8–8.4%.

These figures are shown to indicate that the case of combustion occurring primarily above the regenerator led to better

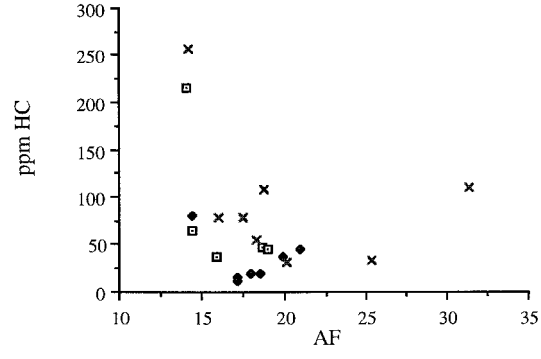

Fig. 5 Comparison of unburned hydrocarbon emissions with AF (airflow 9.6–10.9 kg/h) for all three regenerators. ⊡, 15-ppi ZTA; ♦, 20-ppi mullite; and ×, 300 UCH.

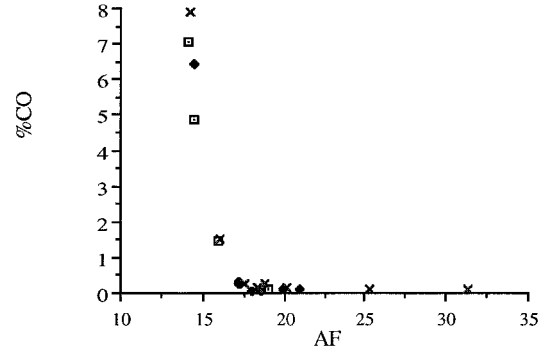

Fig. 6 Comparison of carbon dioxide emissions with AF (airflow 9.6–10.9 kg/h) for all three regenerators. ⊡, 15-ppi ZTA; ♦, 20-ppi mullite; and ×, 300 UCH.

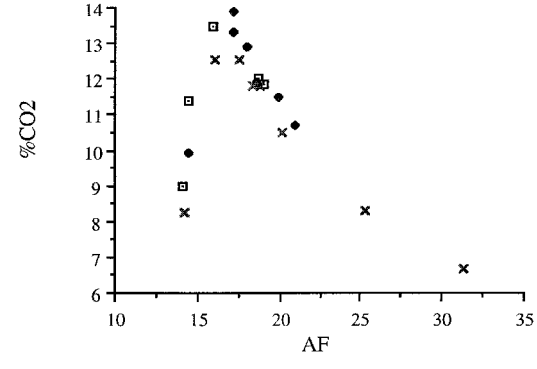

Fig. 7 Comparison of carbon dioxide emissions with AF (airflow 9.6–10.9 kg/h) for all three regenerators. ⊡, 15-ppi ZTA; ♦, 20-ppi mullite; and ×, 300 UCH.

Table 2 Comparison of typical emissions

Engine	%CO	$\%CO_2$	$\%O_2$	Parts per million hydrocarbons
Regenerative (AF 17.2–19.1)				
20-ppi mullite	Below 0.35	11.9–13.2	3.7–5.5	10–40
15-ppi ZTA	Below 0.35	11.6–12.7	3.7–5.4	35–110
300 UCH	Below 0.35	11.8–12.5	3.9–5.3	50–110

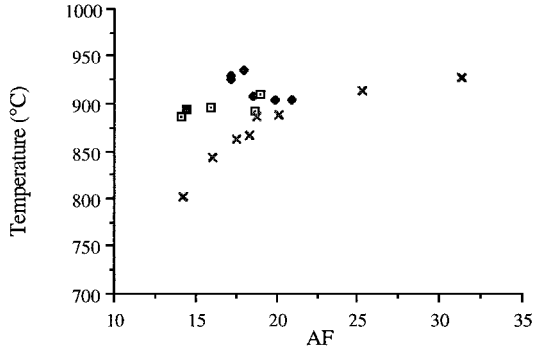

Fig. 8 Comparison of bottom surface temperatures with AF (airflow 9.6–10.9 kg/h) for all three regenerators. ⊡, 15-ppi ZTA; ♦, 20-ppi mullite; and ×, 300 UCH.

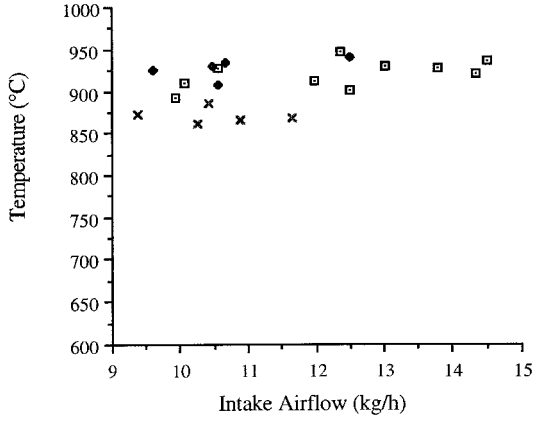

Fig. 9 Comparison of bottom surface temperatures with airflow (AF 17.2–19.1) for all three regenerators. ⊡, 15-ppi ZTA; ♦, 20-ppi mullite; and ×, 300 UCH.

combustion, and also that throttling does not noticeably influence the composition of the exhaust gas.

Next, the effects of lean ignition were studied. Figures 5–7 show a comparison of the three matrices. Combustion at AFs above 20 was possible with unburned hydrocarbon levels below 100 ppm for the 300 UCH and 20-ppi mullite regenerators, respectively. This was probably because of the large reaction surface area of the matrix. These results are unlike those of conventional SI engines, which have unburned hydrocarbon levels rising with AFs above 19. For an SI engine, very lean intake mixtures result in rising unburned hydrocarbon output because the reaction does not reach all regions of the cylinder, leaving part of the intake mixture unreacted.

The data also show a strong dependence of the exhaust composition on AF. Figure 5 indicates unburned hydrocarbons levels to be above 200 ppm for rich intake mixtures (AF < 14.7), with values generally below 100 ppm at lean intake mixtures. Figure 6 shows the typical steep drop-off in CO emissions as the stoichiometric point (AF = 14.7) is passed. Finally, Fig. 7 shows an asymmetric bell-shaped curve with its peak nearly on the stoichiometric point.

Since the 15- and 20-ppi regenerators' cell structure is reticulated, we expected them to outperform the 300 UCH monolith in terms of heat transfer. This is supported by Figs. 8 and 9, where the bottom surface temperature of the 300 UCH monolith was consistently below that of the two reticulated ceramics. Since the hot gas was coming from the top, the temperature of the bottom surface would be proportional to the amount of heat absorbed as the combustion products flowed through it.

A comparison of exhaust gas analysis is shown in Table 2 for intake airflows between 9.6–14.5 kg/h with an AF range of 17.2–19.1. Based on these results, the 20-ppi mullite sample had the best performance. It produced the lowest unburned hydrocarbons emissions, 10–40 ppm, for all three regenerators. The values of %CO for all three matrices are below 0.35%, and the values of $\%CO_2$ are between 11.6–13.2%.

When the three regenerators were examined after testing, no carbon deposits were apparent. It appears that the matrix temperature was high enough to burn off any particulates accumulated on its surface.

The time needed by the 20-ppi mullite matrix to reach self-ignition temperature from ambient was approximately 50 s. The UCH monolith took approximately 1.5–2 min, and the 15-ppi ZTA matrix took a minimum of 5 min. For the ZTA regenerator, it was often necessary to let the engine run with spark ignition for 3–4 min and then reduce the rpm of the engine to increase the contact time of the reactants with the regenerator surface.

Prior to surface ignition of the intake mixture, the combustion origin was a spark located underneath the matrix. As a consequence, the regenerator's bottom surface was directly exposed to the combustion and reached self-ignition temperature (approximately 750°C) before the top face did. At this point the temperature difference between both surfaces was less than 100°C, and the time for the top surface to reach self-ignition temperature was between 3–10 s.

During warm-up the matrix quenched the reaction, resulting in extremely high emissions of unburned hydrocarbons, with values typically above 2000 ppm. When self-ignition did occur, the reaction became nearly complete and unburned hydrocarbon output fell below 100 ppm.

Conclusions

1) Ignition of premixed gasoline and air by a reticulated ceramic surface is possible and can lead to complete and efficient combustion.

2) Complete combustion occurs when surface temperatures are above 1000°C. For our system, the heat release needed to reach these temperatures always resulted in the regenerator matrix top surface temperature being above bottom.

3) The large surface area of the matrix makes complete combustion possible with mass air–fuel ratios above 20.

4) With combustion initiated by the regenerator, carbon particulate buildup did not occur on the regenerator surface under most trials of airflow rate and air–fuel ratio. Only when the matrix surface temperature was too low (<900°C) to initiate combustion did this occur.

Acknowledgments

The authors would like to thank the National Science Foundation for funding this research, Grant CTS-9000574, and they thank the companies that have provided test specimens: Astro-Met Inc., Hi-Tech Ceramics Inc., and Applied Ceramics Inc.

The authors are also grateful to the Briggs and Stratton Corporation for their donation of the test engines.

References

[1]Ruiz, F., and Sepka, S., "New Experiments and Computations on the Regenerative Engine," Society of Automotive Engineers, Paper 930063, March 1993.

[2]Sepka, S., "Experimental Investigations of the Regenerative Engine with Emphasis on Combustion Characteristics," M.S. Thesis, Illinois Inst. of Technology, Chicago, IL, Dec. 1993.

[3]Bone, W. A., and Townend, D., *Flame and Combustion in Gases*, Longmans, Green and Co. Ltd., 1927, pp. 24–55.

[4]Pfefferle, L. D., and Pfefferle, W. C., "Catalysis in Combustion," *Catalysis Reviews. Science and Engineering*, Vol. 29, Nos. 2, 3, 1987, pp. 219–267.

[5]Ramesh, A., Nagalingam, B., and Gopalakrishnan, K. V., "Investigations on the Design and Performance of Two Types of Hot Surface Ignition Engines," Society of Automotive Engineers, Paper 921632, Sept. 1992.

[6]Kesselring, J. P., *Catalytic Combustion, in Advanced Combustion Methods*, edited by J. Weinberg, Academic, London, 1986, pp. 237–275, Chap. 6.

[7]Pischinger, F., Hilger, U., Bartunek, B., Adams, W., and Finsterwalder, G., "Suitability of the Hot-Surface Ignition Engine for Using Alcohol Fuels," VII International Symposium on Alcohol Fuels, Paris, France, Oct. 1986.

[8]Goeckner, B. A., Helmich, D. R., McCarthy, T. A., Arinez, J. M., Peard, T. E., Peters, J. E., Brewster, M. Q., and Buckius, R. O., "Radiative Heat Transfer Augmentation of Natural Gas Flames in Radiant Tube Burners with Porous Ceramic Inserts," *Experimental Thermal and Fluid Science*, Elsevier, Vol. 5, No. 6, 1992, pp. 848–860.

[9]Xiong, T.-Y., Fleming, D. K., and Weil, S. A., *Hazardous Material Destruction in a Self-Regenerating Combustor-Incinerator, Emerging Technologies in Hazardous Waste Management II*, edited by D. W. Tedder and F. G. Pohland, American Chemical Society, Washington, DC, 1991, pp. 12–28.